communications earth & environment

Article

A Nature Portfolio journal

Article in Press

https://doi.org/10.1038/s43247-026-04216-1

Contrasting ecological patterns across deglaciating Western Antarctic Peninsula fjords revealed by soft-sediment benthic assemblages

Check for updates

Miguel Bascur[1,2] ✉, Stuart Jenkins[3], Michael P. Meredith[4], Katy Sheen[5], Carlos P. Muñoz–Ramírez[6], Kate Retallick[3], Antonio Brante[7,8], João Gil[9], Conxita Avila[1,2] & David KA Barnes[4]

Antarctic fjords are natural laboratories for assessing how global change and glacier retreat reshape marine benthic ecosystems, yet comparative studies integrating multiple components of soft-sediment assemblages remain scarce. Here, we assess three glacier-influenced fjords of the Western Antarctic Peninsula: Marian Cove, Börgen Bay and Sheldon Cove. Soft-sediment macrofauna and epibenthic megafauna were sampled along fjord-mouth to glacier-terminus gradients and analysed with hydrographic structure, assemblage composition, diversity, density, biomass, functional groups and a model-derived zoobenthic carbon proxy. Hydrographic structure varied from a shallow surface meltwater lens in Marian Cove to subsurface plume signals in Börgen Bay and Sheldon Cove. Assemblage composition shifted with glacier distance and fjord identity. Diversity increased towards fjord mouths, while glacier-terminus assemblages were more restricted; density, biomass, richness and carbon-storage potential showed non-linear or fjord-specific responses. These findings reveal deglaciating Antarctic fjords as mosaics of benthic ecological assemblages that may vary with local hydrographic and sedimentary settings, and provide a valuable baseline for future studies assessing temporal change in a warming Antarctica.

Antarctic coastal ecosystems are experiencing rapid physical transformations, especially along the Western Antarctic Peninsula (WAP), where reductions in sea ice, instability of ice shelves, glacier retreat and shifts in oceanographic conditions are altering fjord and nearshore habitats[1–7]. In glacial fjords, the retreat of ice exposes seafloor areas that were previously covered by ice[8,9], while meltwater discharge modifies turbidity, sediment delivery and the structure of the water column[10–12]. These environments offer natural opportunities to compare variation in benthic assemblages across glacier-influenced coastal gradients.

Glacial fjords are land-ocean interface systems in which retreating ice and meltwater discharge modify coastal environmental gradients[9,13,14]. Along the WAP, many fjords are fed by marine-terminating glaciers that have retreated markedly in recent decades[4], generating hydrographic and sedimentary gradients that influence how glacier-derived disturbance and particulate material are transferred to the seabed[10,11]. The influx of cold, sediment-laden meltwater can decrease salinity and temperature while increasing turbidity and sedimentation, thereby restricting the diversity of species able to colonise and persist on the seabed[12,15]. At the same time, these newly exposed habitats may be colonised by benthic organisms, providing opportunities to investigate early colonisation and ecological responses to abrupt environmental change in situ[16–18]. Because benthic assemblages in Antarctic fjords can accumulate substantial biomass and organic carbon,

[1]Departament de Biologia Evolutiva, Ecologia i Ciències Ambientals, Facultat de Biologia, Universitat de Barcelona, Barcelona, Spain. [2]Institut de Recerca de la Biodiversitat, Facultat de Biologia, Universitat de Barcelona, Barcelona, Spain. [3]School of Ocean Sciences, Bangor University, Bangor, Gwynedd, UK. [4]British Antarctic Survey, Cambridge, UK. [5]Penryn Campus, University of Exeter, Cornwall, UK. [6]Instituto de Entomología, Universidad Metropolitana de Ciencias de la Educación, Santiago, Chile. [7]Departamento de Ecología, Facultad de Ciencias, Universidad Católica de la Santísima Concepción, Concepción, Chile. [8]Centro de Investigación en Biodiversidad y Ambientes Sustentables (CIBAS), Universidad Católica de la Santísima Concepción, Concepción, Chile. [9]Centre of Marine Sciences (CCMAR), University of Algarve, Campus de Gambelas, Faro, Portugal. ✉e-mail: mbascuba7@alumnes.ub.edu

alterations in their structure are likely to affect not only local biodiversity but also ecosystem functioning and blue-carbon dynamics[19–21]. However, the ecological expression of glacier retreat is unlikely to be uniform among fjords, because meltwater delivery, plume structure, basin geometry and water-mass exchange can modify how the signals of glacial forcing reach the seabed[12,22]. Identifying biological descriptors of these fjord-specific responses is therefore important for monitoring Antarctic coastal change.

Studies in Arctic glacial fjords have shown that soft-sediment benthic assemblages are strongly influenced by glacier-derived sedimentation, physical disturbance and food-supply gradients, often with reduced diversity or functional complexity near glacier fronts and more diverse assemblages towards outer fjord sectors[23,24]. These Arctic systems provide useful high-latitude analogues, but comparable simultaneous, multi-fjord, grab-based assessments of Antarctic soft-sediment benthic fauna remain scarce. In Antarctic fjords, megafaunal assemblages have been documented primarily through seafloor imagery, providing valuable insights into the most conspicuous ecosystem components[15,17,25,26]. These studies show that selected benthic faunal components, such as megafauna or ascidian-dominated assemblages, can provide useful descriptors of glacier-retreat impacts. However, several components of soft-sediment benthic assemblages remain poorly quantified in fjords influenced by retreating marine-terminating glaciers, with few exceptions[27]. This gap is relevant because soft-sediment fauna contributes to sediment reworking, nutrient cycling and energy transfer and therefore plays a central role in benthic ecosystem functioning[28,29]. By integrating multiple components of these assemblages, direct sampling can complement image-based approaches by capturing additional constituents of soft-sediment assemblages. Nevertheless, most existing research has focused on individual fjords, examined only a restricted portion of the benthic assemblage, and often employed limited taxonomic resolution. Yet, despite growing interest in Antarctic blue carbon, the extent to which glacier-influenced variation in soft-sediment assemblages translates into variation in zoobenthic carbon remains poorly resolved, particularly in comparative fjord settings[9,21].

To address this gap, this study investigated biological and environmental variability in three Antarctic fjords along the Western Antarctic Peninsula (WAP). The objectives were to: (i) characterise the water-column properties in each fjord and identify hydrographic signals associated with glacial melt at the time of sampling, (ii) assess benthic assemblage structure and composition along a distance-to-glacier gradient, and (iii) examine how a model-derived zoobenthic carbon proxy (zC proxy) varies along the distance-to-glacier gradient and how it relates to key attributes of benthic assemblage structure. We hypothesised that benthic assemblage composition would shift along the distance-to-glacier gradient, and that density, richness and diversity would generally decrease from fjord mouths to glacier-terminus stations. We further hypothesised that the model-derived zC proxy would increase with distance from the glacier, consistent with higher diversity and structural complexity under weaker glacier influence. To test these hypotheses, soft-sediment benthic assemblages (macrofauna and epibenthic megafauna) were surveyed using a Hamon grab at five stations per fjord across three WAP fjords with documented glacier retreat (Fig. 1). This study provides a multi-fjord comparative assessment of soft-sediment benthic fauna across Antarctic fjords with retreating glaciers, comparing contrasting water-column structures with assemblage composition, biodiversity, functional organisation and carbon-related dimensions of benthic assemblage variation. The resulting baseline provides a comparative framework for assessing how soft-sediment biodiversity, ecosystem functioning and carbon-storage potential vary across glacier-influenced Antarctic coastal habitats.

Results

Hydrographic structure across fjord gradients

Transmittance (%) section plots revealed distinct differences among fjords along the distance-to-glacier gradient (sampling stations 5–1). In Marian Cove (MC), low transmittance was restricted to a shallow surface layer (approximately 10–15 m), below which values were higher and more homogeneous (Fig. 2A). In Börgen Bay (BB; Fig. 2B) and Sheldon Cove (SC; Fig. 2C), minimum transmittance values occurred at intermediate depths (BB: ~40–150 m; SC: ~100–180/200 m), were more pronounced near glacier termini, and weakened towards fjord mouths. This signal was more laterally continuous in SC, whereas BB showed greater heterogeneity and higher transmittance at the fjord-mouth station (BB1).

Salinity section plots also demonstrated contrasting vertical structures among fjords. In MC, a thin low-salinity surface layer (approximately 10–30 m) overlaid a shallow halocline, below which salinity was relatively uniform (Fig. 2D). In BB (Fig. 2E) and SC (Fig. 2F), salinity gradients extended over broader depth ranges (BB: ~80–150 m; SC: ~150–200 m) and transitioned more gradually to saline waters, indicating greater vertical mixing. This stratification was most pronounced in SC. In BB, the fjord-mouth station exhibited higher salinity in the upper and middle water column (~0–150 m) than glacier-proximal stations, indicating along-fjord salinity differences.

Potential temperature (θ, °C) and fluorescence further distinguished the fjords. MC displayed shallow thermal stratification, with warmer surface waters overlying cooler subsurface waters and more uniform conditions at depth (Supplementary Fig. 1A). BB showed colder waters largely confined to a thin surface layer and more homogeneous deeper waters (Supplementary Fig. 1B), whereas SC had a colder upper and intermediate layer extending deeper and more continuously along the fjord (Supplementary Fig. 1C). Fluorescence was concentrated in a shallow surface layer in MC, was weaker and more vertically restricted in BB, and formed a broader near-surface and subsurface maximum across the gradient in SC (Supplementary Fig. 1D–F).

Potential temperature–salinity (θ–S) diagrams corroborated these interpretations. MC occupied a relatively narrow temperature–salinity range, with a slightly fresher surface layer overlying more uniform deeper water, consistent with a shallow stratified meltwater lens (Supplementary Fig. 2A). In contrast, BB and SC exhibited broader temperature–salinity ranges and stronger mixing between cold, fresh glacial meltwater and warmer, saltier deep water (Supplementary Fig. 2B, C). When coloured by beam transmittance, the most turbid waters in MC occurred in the fresher surface branch, whereas in BB and SC they occurred at intermediate densities and depths, consistent with the interpretation that glacial plumes in these latter fjords were expressed mainly as subsurface, vertically mixed layers rather than as a thin surface cap (Supplementary Fig. 2D–F). These hydrographic patterns represent a summer snapshot of conditions at the time of sampling; water-column structure and fluorescence in WAP fjords can vary seasonally and interannually with meltwater discharge, sea-ice cover, vertical mixing and the timing, intensity and duration of phytoplankton blooms, and may also differ with latitude along the WAP.

Benthic assemblage composition along the distance-to-glacier gradient

A total of 5725 individuals (19,084 ind. m^{-2}) were recorded across the three fjords, representing 22 higher taxonomic groups, 9 phyla and 216 morphospecies. Species overlap among our fjord samples was limited, with only 34 morphospecies (15.7%) shared by Marian Cove, Börgen Bay and Sheldon Cove (Supplementary Fig. 3A). Taxa recorded only in one fjord within our samples accounted for 54 morphospecies in Marian Cove (25.0%), 47 in Sheldon Cove (21.8%) and 28 in Börgen Bay (13.0%). Pairwise observed overlap was highest between Börgen Bay and Sheldon Cove (30 morphospecies; 13.9%), followed by Marian Cove and Börgen Bay (13; 6.0%), and lowest between Marian Cove and Sheldon Cove (10; 4.6%). Although these observations suggest limited taxonomic overlap among the sampled fjord assemblages, species accumulation curves remained positively sloped at maximum sampling effort in all three fjords, indicating incomplete inventories (Supplementary Fig. 3B). Observed richness was 105–121 taxa per fjord, whereas Chao1 and Chao2 estimated 180.1–217.3 and 194.2–236.3 taxa, respectively, corresponding to 51.1–67.2% and 51.2–54.1% observed-to-estimated completeness. Incidence-based coverage ranged from 0.813 to 0.881, and terminal accumulation rates remained positive (1.67–2.36 taxa per sample). Therefore, taxa recorded only in a single fjord should be

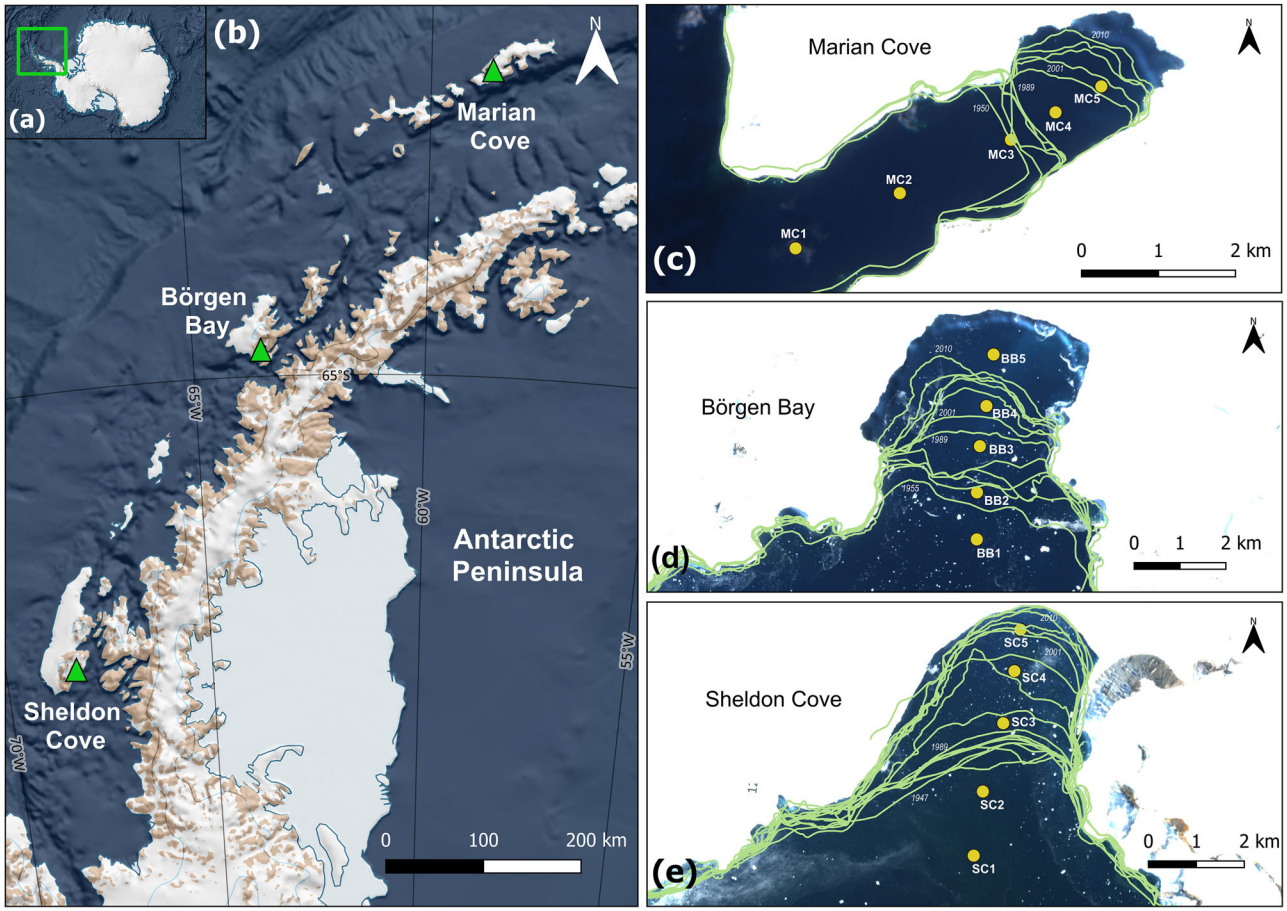


Fig. 1 | Location of the studied fjords. a Map of the Antarctic continent highlighting the Antarctic Peninsula. **b** Location of the three fjords examined along the Western Antarctic Peninsula (WAP). Sampling stations (yellow dots) within each fjord are shown in (**c**) Marian Cove, King George Island (62°S; MC1–MC5); **d** Börgen Bay, Anvers Island (64°S; BB1–BB5); and **e** Sheldon Cove, Adelaide Island (67°S; SC1–SC5). **e** shows the inner Sheldon Cove sampling area near the Sheldon Glacier; the full cove extends approximately 13.5 km. In all panels, estimated historical glacier retreat lines are shown in green[90]. Basemaps in (**a, b**) were elaborated in QGIS (v3.44.1) using the Quantarctica package (v3.2). Satellite images at 10 m resolution for (**c–e**) were obtained from Sentinel−2 via the Copernicus Open Access Hub and processed in QGIS. Copernicus imagery dates are 24 October 2024 for MC, 23 February 2019 for BB and 18 January 2020 for SC.

interpreted as fjord-specific within the present sampling rather than as evidence of ecological or biogeographical exclusivity, and actual taxonomic overlap among fjords may be greater than indicated by the observed records (Supplementary Table 1).

Gross taxonomic-group composition. Polychaetes constituted the dominant group in terms of density across all fjords, while the identity of co-dominant groups varied along the distance-to-glacier gradient. In Marian Cove, a transition was observed from polychaete dominance at the fjord mouth to increased contributions from bivalves and ascidians at inner stations. Börgen Bay remained predominantly polychaete-dominated, except at a mid-fjord station where actinarians were most abundant. In contrast, Sheldon Cove displayed a more balanced distribution among polychaetes, bivalves and actinarians, with actinarians becoming most prominent near the glacier terminus (Supplementary Fig. 4A). Biomass patterns, unlike density patterns, were primarily influenced by large-bodied taxa such as ophiuroids, ascidians, asteroids and actinarians, resulting in fjord-specific biomass structures that diverged from density-based dominance patterns (Supplementary Fig. 4B).

Variation in taxonomic assemblage composition. Permutational multivariate analysis of variance (PERMANOVA) based on Bray–Curtis dissimilarities demonstrated that benthic assemblage composition differed significantly among fjords, along the distance-to-glacier gradient, and through their interaction (Table 1). Fjord identity accounted for 25% of the multivariate variance (pseudo-$F = 20.998$, $p < 0.001$), while distance to the glacier explained 17.2% (pseudo-$F = 7.217$, $p < 0.001$). The interaction between fjord and distance contributed an additional 19.8% (pseudo-$F = 4.149$, $p < 0.001$), indicating substantial regional differences as well as fjord-specific responses to glacial proximity. These patterns were evident in the principal coordinates analysis (PCoA) ordination plot (Fig. 3A). Samples clustered according to fjord, with further separation among distance groups within each fjord. Stations located near the glacier terminus generally occupied more extreme positions in ordination space. In contrast, intermediate and outer stations formed tighter clusters, suggesting a shift in assemblage structure with increasing distance from the glacier terminus. Species vectors overlaid on the PCoA identified a limited set of taxa driving these gradients. *Nuculana inaequisculpta* was associated with the Marian Cove cluster, while *Thyasira debilis*, *Lumbrineris kerguelensis* and Edwardsiidae gen. sp. 1 were characteristic of the Börgen Bay and Sheldon Cove groups. Along the distance-to-glacier gradient, *Terebellides kerguelensis* and *Maldane sarsi antarctica* were linked to external stations of the fjords, whereas Edwardsiidae gen. sp. 1 and *Thyasira debilis* were associated with stations near the glacier terminus, particularly in Börgen Bay and Sheldon Cove.

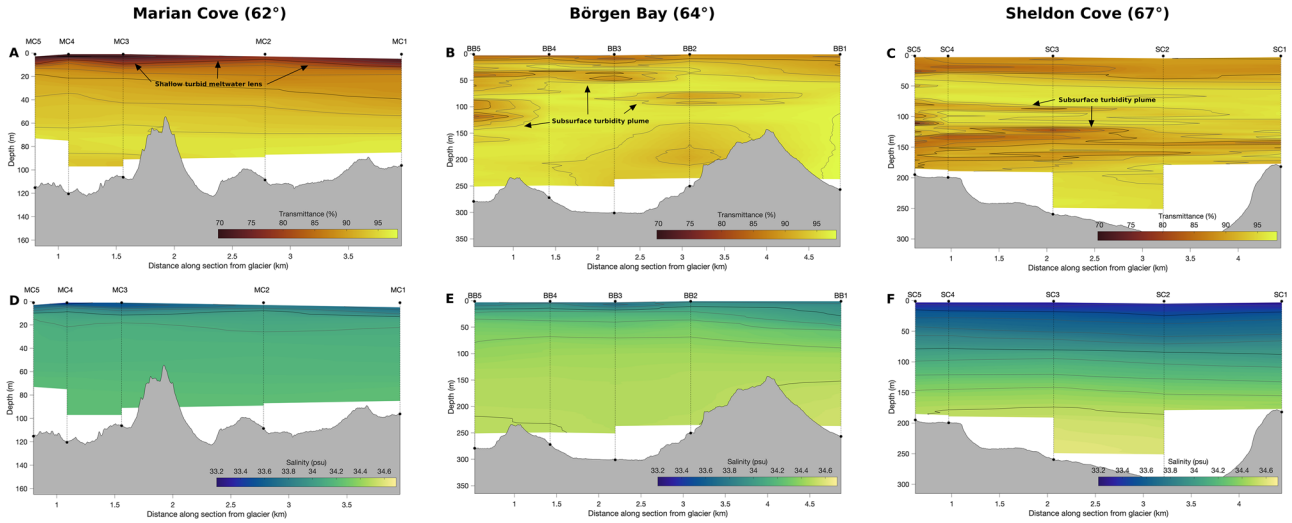


Fig. 2 | Along-fjord section plots of transmittance (%) and salinity (psu) from the glacier front (left) to the fjord mouth (right) for the three studied fjords along the Western Antarctic Peninsula (WAP). A–C present transmittance for Marian Cove, Börgen Bay and Sheldon Cove, respectively, and panels D–F show the corresponding salinity sections. Sampling stations are marked in the upper section of each plot. The y-axis indicates depth (*m*), and the grey shading represents the bathymetric profile along each transect. Black contours show the main isolines, whereas grey contours show intermediate intervals. In the transmittance sections, black contours are drawn every 10% and grey contours every 2.5%; in the salinity sections, black contours are drawn every 0.5 psu and grey contours every 0.125 psu.

Pairwise PERMANOVA results, summarised in the heatmaps (Fig. 3B, C and Supplementary Tables 2, 3), confirmed that many distance groups differed significantly within each fjord and that these differences were particularly marked in Börgen Bay and Sheldon Cove, where effect size (R^2) values were often ≥0.4. In Marian Cove, the observed gradient was present but less pronounced. Several contrasts among intermediate distances were not statistically significant, suggesting a more gradual shift in assemblage composition along the transect. Comparisons across fjords revealed that assemblages at equivalent distances from the glacier differed significantly in nearly all cases. The R^2 values for these differences ranged from moderate to high, typically between 0.35 and 0.56, showing that assemblages exposed to similar degrees of glacial influence can still diverge substantially depending on the fjord in which they occur.

Key taxa driving assemblage composition differences. SIMPER-based boxplots indicated that assemblage composition was primarily driven by shifts in the densities of a limited number of taxa at specific locations (Supplementary Fig. 5 and Supplementary Tables 4, 5). Within fjords, comparisons between mouths and glacier termini revealed pronounced density contrasts and presence–absence patterns. In Marian Cove, *Maldane sarsi antarctica*, *Amythas membranifera* and *Terebellides kerguelensis* were most abundant at the fjord mouth, whereas *Amphitrite kerguelensis* and *Perkinsiana antarctica* reached their highest densities near the terminus. In Börgen Bay and Sheldon Cove, most retained SIMPER taxa were largely restricted to fjord-mouth stations and were rare or were not detected near glacier termini (Supplementary Fig. 5A–C).

Comparisons among glacier-terminus stations revealed distinct assemblages within each fjord. The Marian Cove terminus exhibited high densities of *Amphitrite kerguelensis*, *Perkinsiana antarctica* and Ascidiacea gen. sp. 7. In contrast, the Börgen Bay terminus was characterised by *Amphicteis antarctica*, *Pseudokellya franki* and several tube-dwelling polychaetes. At the Sheldon Cove terminus, *Edwardsia* sp., Edwardsiidae gen. sp. 1, *Echiurus antarcticus* and *Lumbrineris kerguelensis* were predominant. Total Bray–Curtis dissimilarity between selected site pairs was high (80–99%), with retained SIMPER taxa showing marked density contrasts among polychaetes, bivalves and actinarians (Supplementary Fig. 5D–F).

The complementary bubble plot summarised changes in the relative density of the five most abundant benthic taxa at each station along the fjord gradients (Fig. 4). In Marian Cove, *Maldane sarsi antarctica* was prominent at the fjord mouth, while *Nuculana inaequisculpta* remained among the dominant taxa across the transect and *Amphitrite kerguelensis* and ascidians became more abundant towards the glacier terminus (Fig. 4A). In Börgen Bay, deposit-feeding polychaetes dominated the fjord mouth, whereas Edwardsiidae spp., *Thyasira debilis* and *Nuculana inaequisculpta* characterised intermediate to inner stations, with *Amphicteis antarctica* and *Pseudokellya franki* among the leading taxa at the glacier terminus (Fig. 4B). In Sheldon Cove, *Thyasira debilis* and *Edwardsia* sp. were prominent at the fjord mouth, whereas Edwardsiidae spp. and bivalves became more abundant at intermediate to inner stations and *Edwardsia* sp. and *Echiurus antarcticus* characterised the glacier terminus (Fig. 4C).

Functional composition of benthic assemblages. The composition and number of functional groups varied along the distance-to-glacier gradient in all three fjords, with each system displaying a distinct pattern (Fig. 5). In Marian Cove, vermiform deposit feeders dominated the fjord mouth, where 12 functional groups were recorded. At mid-fjord stations, shelled burrowers and deposit feeders were most prominent, and the number of functional groups remained stable (10). Near the glacier, the assemblage shifted to a more even distribution among shelled burrowers, deposit feeders, vermiform deposit feeders and sessile suspension feeders (9 groups; Fig. 5A). In Börgen Bay, the fjord mouth was dominated by vermiform deposit feeders, together with crawler deposit feeders and mobile, soft-bodied scavenger/predator taxa (9 groups). Functional-group richness peaked at 3–4 km (12 groups), reached its lowest values at 2–3 km and at the glacier terminus (8 groups), and assemblages towards inner stations consisted of varying mixtures of mobile and sessile soft-bodied scavenger/predator taxa, shelled burrowers, deposit feeders and vermiform deposit feeders (Fig. 5 B). In Sheldon Cove, the fjord mouth exhibited a broad and relatively even combination of functional groups (12 groups). At 3–4 km and 2–3 km, sessile soft-bodied scavenger/predator taxa dominated, although shelled burrowers, deposit feeders, mobile soft-bodied scavenger/predator taxa and vermiform deposit feeders continued to contribute substantially (9–10 groups). At 1–2 km, shelled burrowers and deposit feeders were predominant (10 groups), whereas the glacier terminus was dominated by sessile and mobile soft-bodied scavenger/predator taxa and had the lowest number of functional groups recorded in this fjord (7; Fig. 5C).

Table 1 | Results of sequential permutational multivariate analysis of variance (PERMANOVA), based on Bray-Curtis dissimilarity matrix and fourth-root data transformation, testing for the effect of fjord and distance to the glacier on benthic assemblage composition

Source of variation	df	SS	R^2	pseudo *F*	*P*(perm)
Fjord (*F*)	2	6.659	0.250	20.998	**<0.001**
Distance to glacier (D)	4	4.578	0.172	7.217	**<0.001**
F × *D*	8	5.264	0.198	4.149	**<0.001**
Residual	64	10.149	0.380		
Total	78	26.650	1.000		

Significant results (*P*(perm) < 0.05) are highlighted in bold. *P*-values were obtained using type I sum of squares and 9999 permutations under the full model.
df degrees of freedom, *SS* sum of squares. R^2 values indicate the proportion of multivariate variation explained by each term.

Assemblage structure (density, biomass, richness and diversity) along the distance-to-glacier gradient. Analyses of species richness, total density, biomass, Shannon diversity, Simpson diversity and inverse Simpson diversity revealed distinct spatial patterns along the distance-to-glacier gradient from mouth to glacier terminus (Supplementary Table 6). Species richness and all diversity indices reached their highest values at Sheldon Cove, particularly at the outer stations. In comparison, Börgen Bay and Marian Cove exhibited less diverse assemblages at equivalent distances. Mixed-effects models indicated that distance to glacier termini significantly influenced total density, biomass, Shannon diversity, Simpson diversity and inverse Simpson diversity. Total density and biomass also differed significantly among fjords and significant fjord × distance interactions affected total density, biomass and inverse Simpson diversity, suggesting that benthic assemblage patterns varied among fjords (Table 2). Patterns of density and biomass were non-linear: in Sheldon Cove, biomass displayed an inverse relationship, with low values near the glacier and a consistent increase towards the fjord mouth. In contrast, Marian Cove and Börgen Bay exhibited more irregular variation in biomass and total density along the gradient (Fig. 6A, B). Species richness models did not reveal significant differences with distance to the glacier across the three fjords, in contrast to the diversity indices and aggregate measures of density and biomass (Fig. 6C). Conversely, models for Shannon, Simpson and inverse Simpson diversity demonstrated linear trends, with diversity increasing consistently with greater distance from the glacier terminus across all three fjords (Fig. 6D–F). A full table of cumulative densities across replicates for each morphospecies at each distance-to-glacier station and within each fjord is presented in Supplementary Table 7.

Variation of the model-derived zC proxy along distance-to-glacier and species-richness gradients

The model-derived zC proxy varied significantly along the distance-to-glacier gradient (Fig. 7A and Supplementary Table 6), with distance from the glacier terminus identified as the only significant predictor. The mixed-effects model revealed a non-linear relationship: zC proxy was lowest at stations nearest the glacier terminus, reached its highest values at intermediate distances, and declined again towards the fjord mouth (Table 2). In parallel, zC proxy was positively associated with taxonomic richness (Fig. 7B). In the richness models, taxonomic richness was the only significant predictor of variation in zC proxy. Model results indicated that zC proxy increased with richness, with a tendency to plateau at the upper end of the richness gradient. The absence of significant interactions in both models suggests that these relationships were broadly consistent among fjords and along both the distance-to-glacier and species-richness gradients.

Discussion

Our comparison of Marian Cove, Börgen Bay and Sheldon Cove indicates that glacial influence is associated with both shared and fjord-specific benthic responses across Western Antarctic Peninsula fjords. Assemblage composition changed significantly along the distance-to-glacier gradient in all three systems, and diversity consistently increased towards fjord mouths. However, density, biomass, richness and the model-derived zC proxy exhibited non-linear or fjord-specific responses, indicating that glacial influence did not generate a single uniform benthic pattern. Consequently, the initial hypotheses were only partially supported; rather than a simple decline of benthos towards glacier termini, glacier influence was associated with shifts in dominance, evenness, functional structure and carbon-storage potential. These findings align with previous studies indicating that rapidly deglaciating Antarctic systems can experience substantial change in benthic structure without following uniform ecological patterns[15,17,26].

Hydrographic and sedimentary context along fjord gradients

Oceanographic structure varied markedly among the three fjords, suggesting that glacial influence may have been represented through the water column in different ways. Marian Cove exhibited a shallow, fresh and turbid surface layer, consistent with a surface meltwater lens from a predominantly land-terminating glacier. Elevated transmittance below this layer suggests limited direct summer glacial influence on deeper waters, although seasonal mixing and restricted exchange may transfer surface signals to the seabed over longer periods[30,31]. This surface-concentrated glacier signal may help explain the more gradual benthic turnover observed in Marian Cove.

In contrast, Börgen Bay and Sheldon Cove displayed low-transmittance layers at intermediate depths, characteristic of subsurface plumes associated with marine-terminating glaciers. These plumes are generated when meltwater released at depth rises, entrains ambient saline water and spreads laterally at neutral buoyancy[22,32–35]. By broadening the vertical range of suspended-particle exposure and modifying organic-matter delivery, such plume structures may contribute to the stronger taxonomic differences observed near glacier termini in Börgen Bay and Sheldon Cove. It is important to note that the data presented here were obtained on a single summer expedition, and that hydrography and bloom dynamics can vary on a range of timescales[36,37]. Nonetheless, the intermediate-depth low-transmittance layer seen here has been observed in other years in the same locations, and also in quasi-weekly sampling in Ryder Bay (adjacent to Sheldon Cove), and the hydrographic structures are not atypical in relation to other datasets[38]. Consequently, there would appear to be a reasonable level of representativeness on interannual timescales, at least in relation to the physical and biogeochemical properties observed. It is accepted, however, that systematic observations of sedimentation, seabed sediment properties and organic-matter measurements would be needed to fully address the issue of persistence and mechanistic influence of the conditions on benthic assemblage structure.

Glacier-derived hydrographic signals may influence benthic habitats through the transport and deposition of suspended material. Therefore, sedimentary conditions offer essential complementary context for interpreting observed assemblage patterns. Additional ^{210}Pb-derived sediment-accumulation data from the same fjord systems provide useful context, although they are not spatially matched to all biological stations of the present work[39]. In Marian Cove, the highest sediment accumulation rate was recorded at the fjord mouth rather than near the glacier terminus, consistent with a more spatially decoupled transfer of glacier-derived material to the seabed. In contrast, Börgen Bay showed the highest value overall at a station near the glacier terminus, consistent with stronger benthic exposure to suspended particles under the observed subsurface low-transmittance layer. For Sheldon Cove, only one sediment-accumulation station was available, so sedimentation cannot yet resolve a full distance-to-glacier gradient. These data therefore support sediment delivery and habitat stability as plausible contributors to fjord-specific benthic ecological patterns.

Stable-isotope evidence from Marian Cove and Sheldon Cove provides independent evidence for fjord-specific differences in benthic resource

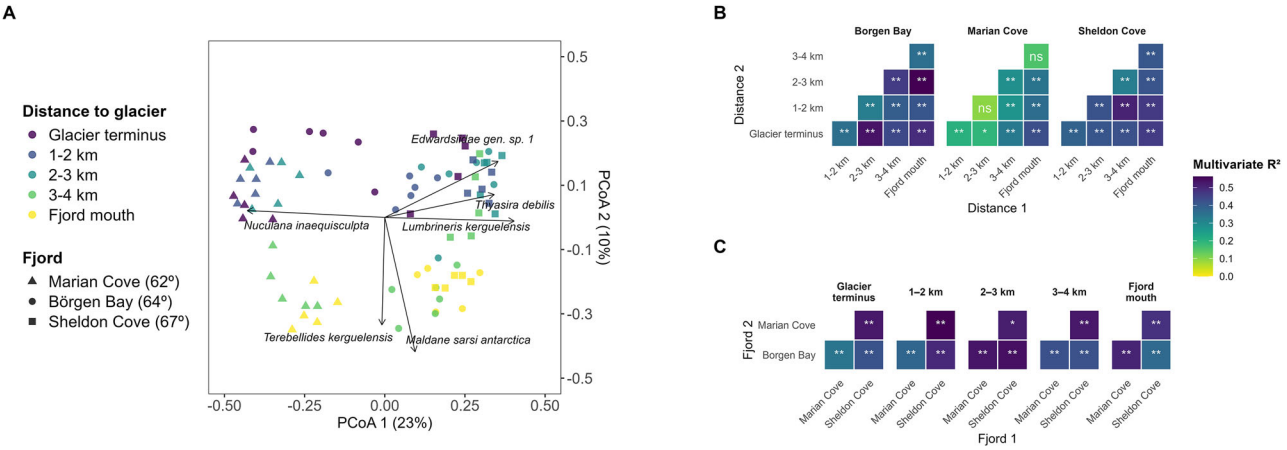


Fig. 3 | Principal coordinate analysis (PCoA) of benthic assemblage composition based on Bray-Curtis distance metric (**A**) and heatmaps summarising pairwise multivariate differences, after PERMANOVA statistics, among distance classes within each fjord (**B**) and among fjords at each distance class (**C**) along the distance-to-glacier gradient at the three studied fjords. In panel A, arrows represent the main contributing species, with arrow direction showing the gradient of increasing abundance and arrow length indicating the strength of their association with the ordination axes. Heatmaps show effect sizes based on multivariate R^2, and levels of significance are also indicated (**$p < 0.001$; *$p < 0.01$; ns = non-significant). Analyses were based on $n = 79$ independent grab samples: Marian Cove, $n = 25$; Börgen Bay, $n = 29$; Sheldon Cove, $n = 25$.

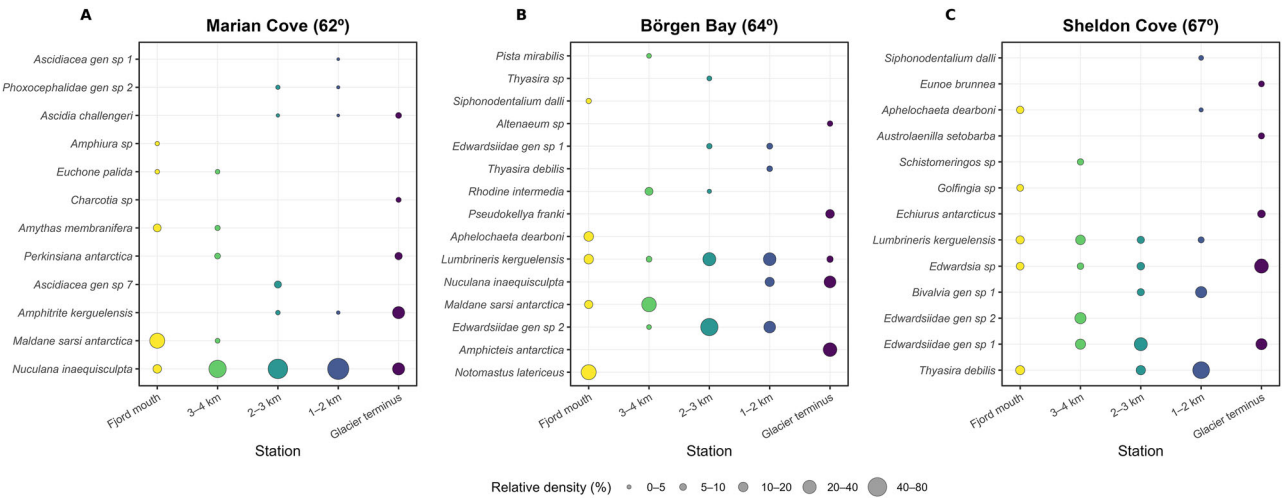


Fig. 4 | Bubble plot showing the relative density of the five most abundant benthic taxa at each station along the distance-to-glacier gradient in Marian Cove (**A**), Börgen Bay (**B**) and Sheldon Cove (**C**) along the Western Antarctic Peninsula (WAP). Bubble size is proportional to relative density.

pathways[40]. *Nuculana inaequisculpta* was ^{13}C-depleted near the land-terminating Fourcade Glacier in Marian Cove, whereas *Edwardsia* sp. was ^{13}C-enriched near the marine-terminating Sheldon Glacier in Sheldon Cove. This contrast suggests that dominant benthic consumers in the two fjords utilised distinct basal resources and/or carbon pathways under glacier influence[40]. Resource utilisation appears to differ between a system with a shallow surface meltwater lens and one where plume-related signals are more pronounced at subsurface depths. Although these isotope patterns do not directly identify the mechanisms shaping assemblage structure, they support the interpretation that fjord-specific hydrographic and sedimentary conditions may influence bentho-pelagic coupling, particle delivery and carbon transfer to the seabed[41–44].

Shifts in structure and composition of benthic assemblages

The benthic response along the fjord gradient did not manifest as a simple linear decline in abundance towards glacier termini. Instead, it involved a shift in assemblage structure. Diversity indices increased towards fjord mouths across all three systems, while richness, density and biomass exhibited non-linear or fjord-specific patterns. These findings suggest that glacial influence primarily altered dominance structure and evenness, rather than causing straightforward taxon loss. Near the glacier termini, a limited number of tolerant taxa contributed disproportionately to abundance and biomass. In contrast, assemblages at outer stations were more balanced, a pattern also observed in other polar fjords experiencing glacier-derived disturbance[15,17,23].

Multivariate analyses demonstrated that benthic turnover was influenced by both glacier proximity and fjord-specific environmental conditions. Polychaetes remained important across all fjords; however, the identity of co-dominant groups varied substantially. These differences were expressed primarily through shifts in dominance rather than complete taxonomic replacement. Sharper transitions in Börgen Bay and Sheldon Cove suggest stronger ecological filtering, while the more gradual pattern in Marian Cove aligns with a weaker or more diffuse transfer of glacial forcing to the seabed. These findings support the view that Antarctic fjords do not display a uniform spatial pattern of ecological change along deglaciation gradients, but instead develop distinct ecological responses depending on the interplay of meltwater input, sedimentation and habitat stability within each basin[15,17,45]. As accumulation curves and Chao estimators suggest that

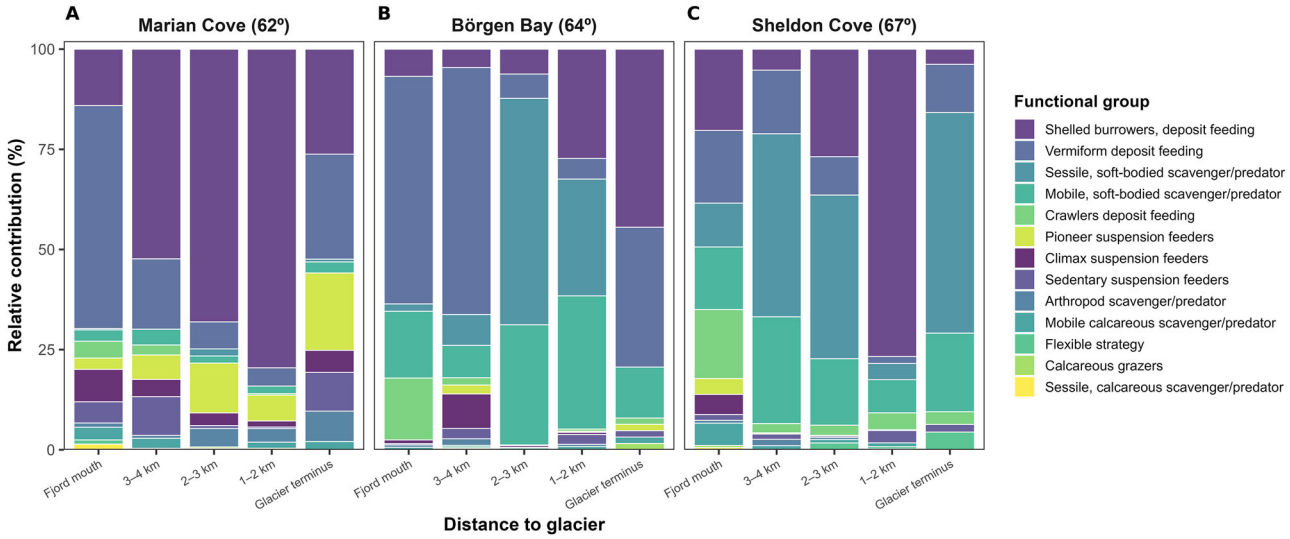


Fig. 5 | Relative contribution of different functional groups[9] to benthic assemblages along the distance-to-glacier gradient in Marian Cove (**A**), Börgen Bay (**B**) and Sheldon Cove (**C**) along the WAP.

fjord-level inventories remain incomplete, the observed fjord-specific taxa should be interpreted with caution and not regarded as definitive evidence of ecological exclusivity. The higher abundance-based coverage (0.96–0.98) than incidence-based coverage (0.81–0.88) indicates that the dominant assemblage components were sampled more thoroughly than the full pool of taxa occurring across replicate samples. Consequently, further sampling would likely detect additional low-frequency taxa, potentially increasing the observed overlap among fjords, while exerting less influence on abundance-based compositional differences driven by recurrent and numerically dominant taxa.

The observed assemblage patterns along fjords may reflect not only an inferred difference in exposure of the seabed following glacier retreat but also contemporary environmental filtering. Distance from glacier termini serves as a (non-linear) proxy for seafloor exposure duration after ice retreat, but may also covary with sediment properties, sediment stability, oxygen availability and benthic food supply. In soft-sediment systems, factors such as granulometry, sedimentation vs. sediment accumulation rates, organic enrichment, redox conditions and the quantity and quality of phytodetrital inputs can significantly influence faunal diversity and species composition[46–51]. Consequently, the pronounced assemblage shifts observed in Börgen Bay and Sheldon Cove may be attributed not only to differences in habitat exposure, but also to more intense filtering by sediment delivery, habitat instability and organic-matter pathways. As these variables were not included as formal predictors in this study, this interpretation remains plausible but untested, highlighting that hydrography alone cannot fully resolve the mechanisms driving benthic assemblage structure and that future studies should integrate spatially matched biological and environmental matrices across Antarctic fjord gradients.

Turnover was primarily driven by changes in a limited set of key taxa. Stations located farther from the glacier were consistently associated with deposit-feeding polychaetes, including *Terebellides kerguelensis* and *Maldane sarsi antarctica*. These species typify stable soft-sediment assemblages and have also been documented in outer fjord habitats in other polar systems[52,53]. In contrast, stations near the glacier terminus, particularly in Börgen Bay and Sheldon Cove, were characterised by edwardsiid anemones and small bivalves such as *Thyasira debilis*, which are indicative of fine, unstable sediments under persistent glacier influence. Marian Cove exhibited a different pattern, with *Amphitrite kerguelensis* and *Perkinsiana antarctica* present near the glacier terminus. This suggests that glacier-influenced habitats can support fjord-specific assemblage states rather than a single characteristic fauna.

Functional composition reflected these taxonomic changes, indicating that glacier influence may have acted as an ecological filter[11]. Marian Cove maintained relatively high functional-group richness along the transect. In contrast, Börgen Bay and Sheldon Cove exhibited greater functional simplification towards the glacier, with increased dominance of mobile and sessile soft-bodied scavenger/predator groups. Similar reductions in functional complexity under chronic glacial disturbance have been documented in both Arctic and Antarctic fjords[20,54]. This agreement with findings from Arctic fjord studies supports the broader relevance of glacier-derived sedimentation and physical disturbance as structuring forces in high-latitude soft-sediment benthic systems, while also highlighting the need for region-specific Antarctic assessments.

Comparisons with Potter Cove, Marian Cove and Sheldon Cove underscore the broader significance of these findings. Previous studies have associated glacier retreat and increased sediment input with transitions from filter-feeder or ascidian-dominated assemblages to more opportunistic, deposit-feeding or pioneer taxa in newly exposed or unstable habitats[15,17,21,26,45]. In this spatial snapshot, the distance-to-glacier gradients are best interpreted as spatial differences in assemblage structure likely associated with sedimentation, habitat stability and bentho-pelagic coupling, rather than as simple linear successional sequences. Under stronger glacier influence, assemblages were more selective, less even and functionally simplified. In contrast, under weaker or more decoupled disturbance, assemblages were more balanced and diverse.

Model-derived zoobenthic carbon proxy (zC proxy) patterns

The model-derived zC proxy exhibited a statistically significant spatial pattern along the distance-to-glacier gradient, with distance from the glacier identified as the sole significant predictor. The optimal quadratic model revealed the lowest values near glacier termini, peak values at intermediate distances and reduced values towards fjord mouths. This hump-shaped pattern is consistent with two non-mutually exclusive mechanisms. First, intermediate stations may serve as zones where reduced glacier disturbance and partial seabed stabilisation facilitate the development of higher biomass, species richness, or functional complexity. Second, the pattern aligns with the Intermediate Disturbance Hypothesis, which posits that intermediate levels of physical disturbance promote greater diversity or coexistence compared to either highly disturbed glacier-proximal habitats or less disturbed outer-fjord habitats[55]. In this context, the mid-fjord zC peak likely results from the combined effects of disturbance intensity, habitat stability and the local dominance of functional groups with higher zC coefficients, rather than a single successional pathway.

Table 2 | Statistical summary of linear and non-linear mixed-effect models (LME, NLME) for density, biomass, diversity and the zoobenthic carbon proxy (zC) parameters and generalised linear mixed-effect models (GLMM) for species richness compared between fjords and across sampling stations within fjords at different distances from retreating glaciers

Source of variation	df	*F*-value	*p*-value	Marginal R^2
Density				0.59
Fjord = *F*	2	3.32	**0.041**	
Distance to glacier = D	1	45.62	**<0.001**	
F × *D*	2	6.06	**0.004**	
Residuals	72			
Biomass				0.49
Fjord = *F*	2	4.43	**0.015**	
Distance to glacier = *D*	1	9.17	**0.003**	
F × *D*	2	10.14	**<0.001**	
Residuals	72			
Shannon				0.43
Fjord = *F*	2	0.39	0.684	
Distance to glacier = *D*	1	16.18	**0.001**	
F × *D*	2	0.88	0.435	
Residuals	72			
Simpson				0.32
Fjord = *F*	2	1.38	0.283	
Distance to glacier = *D*	1	8.93	**0.009**	
F × *D*	2	0.11	0.896	
Residuals	72			
Inverse Simpson				0.44
Fjord = *F*	2	0.46	0.637	
Distance to glacier = *D*	1	14.45	**0.002**	
F × *D*	2	4.21	**0.034**	
Residuals	72			
Zoobenthic carbon				0.37
Fjord = *F*	2	0.20	0.822	
Distance to glacier = *D*	1	11.94	**0.004**	
F × *D*	2	0.73	0.497	
Residuals	72			
Richness	df	χ^2	*p*-value	0.68
Fjord = *F*	2	0.16	0.922	
Distance to glacier = *D*	1	2.93	0.087	
F × *D*	2	1.17	0.557	

df degrees of freedom, χ^2 Chi-square value. Marginal R^2 represents the variance explained by the fixed effects of each model.

The positive association between the zC proxy and species richness should be interpreted as comparative rather than deterministic. In high-latitude systems, zoobenthic carbon storage or its potential frequently covaries with richness, density, functional diversity and the presence of calcified or habitat-structuring taxa[20,56]. However, species richness alone does not determine carbon accumulation, which is also influenced by body size, degree of calcification, functional structure and substratum type, amongst others. Therefore, higher species richness should not be assumed to indicate greater absolute zoobenthic carbon.

Because the zC proxy applies coefficients beyond their original calibration context, the absolute magnitude of these estimates should be interpreted with caution. The Barnes et al.[9]-derived framework relies on functional-group classifications, literature-derived carbon values and regional zoobenthic datasets, including seabed imagery and benthic material collected with Agassiz trawls[9,21]. However, these coefficients were not specifically calibrated for quantitative grab sampling of soft-sediment macrofaunal and epibenthic assemblages. Overestimation may result when dense assemblages of small-bodied or weakly calcified organisms are converted using coefficients derived from larger or more heavily calcified epifaunal taxa[9,21]. Consequently, zC values are most appropriately interpreted as relative comparisons among stations rather than as absolute carbon-stock estimates.

This uncertainty underscores the need for conversion models specifically tailored to grab-sampled soft-sediment assemblages. A conservative calibration workflow would involve taxon- or trait-specific measurements of dry mass, ash-free dry mass and tissue carbon content from representative grab-collected taxa, estimation of preservation-specific wet-mass conversion factors and uncertainty propagation for biomass-to-carbon coefficients[57,58]. Such calibration would enhance the reliability of faunal biomass and functional composition in polar blue carbon assessments. Additionally, once calibrated, proxy-based approaches could reduce the necessity for destructive carbon analyses of all specimens, thereby preserving valuable benthic material for taxonomic collections, museum deposition and future collaborative studies. More broadly, carbon-related properties differ among habitats, substrata, biological compartments and estimation approaches across Antarctic, sub-Antarctic and other non-polar, coastal blue carbon systems[20,59–62]. This variation reinforces the concept that glacier-influenced fjords are heterogeneous systems in which biodiversity, functional organisation, and carbon-storage potential vary unevenly along glacier-retreat gradients.

Ecological implications for deglaciating Antarctic fjords

The results presented here have important ecological and applied implications for monitoring Antarctic fjords as glacier retreat continues. Glacier retreat should not be assumed to inherently produce more complex habitats or increase carbon-storage potential. Instead, outcomes depend on shifts in benthic assemblage structure under varying disturbance regimes, seabed stability, habitat availability and local hydrographic and geomorphological conditions. In certain sectors, ice loss may promote more complex assemblages, greater biomass and enhanced carbon-storage potential, whereas persistent sediment disturbance or functional simplification may limit these developments.

Consequently, the soft-sediment benthic faunal assemblages provide a complementary biological component, while assemblage composition, diversity/evenness, functional-group structure and the zC proxy provide assemblage-level, functional and carbon-related descriptors of benthic change under ongoing Antarctic deglaciation. These findings support the adoption of a mosaic-based approach to monitoring and conservation in Antarctic fjords, encompassing highly disturbed stations near glacier termini, intermediate zones characterised by strong turnover and fjord-mouth stations where more balanced assemblages and more stable carbon-related properties may develop. This heterogeneity represents a fundamental component of ecological value and spatial planning relevance in polar marine environments, with significant implications for biodiversity conservation and precautionary management frameworks[19,21,56,63]. As Antarctic fjords and marine sediments are increasingly recognised as emerging polar blue carbon systems, robust and standardised ecological baselines will be essential for understanding how biodiversity and carbon-related functions respond to ongoing environmental change[64].

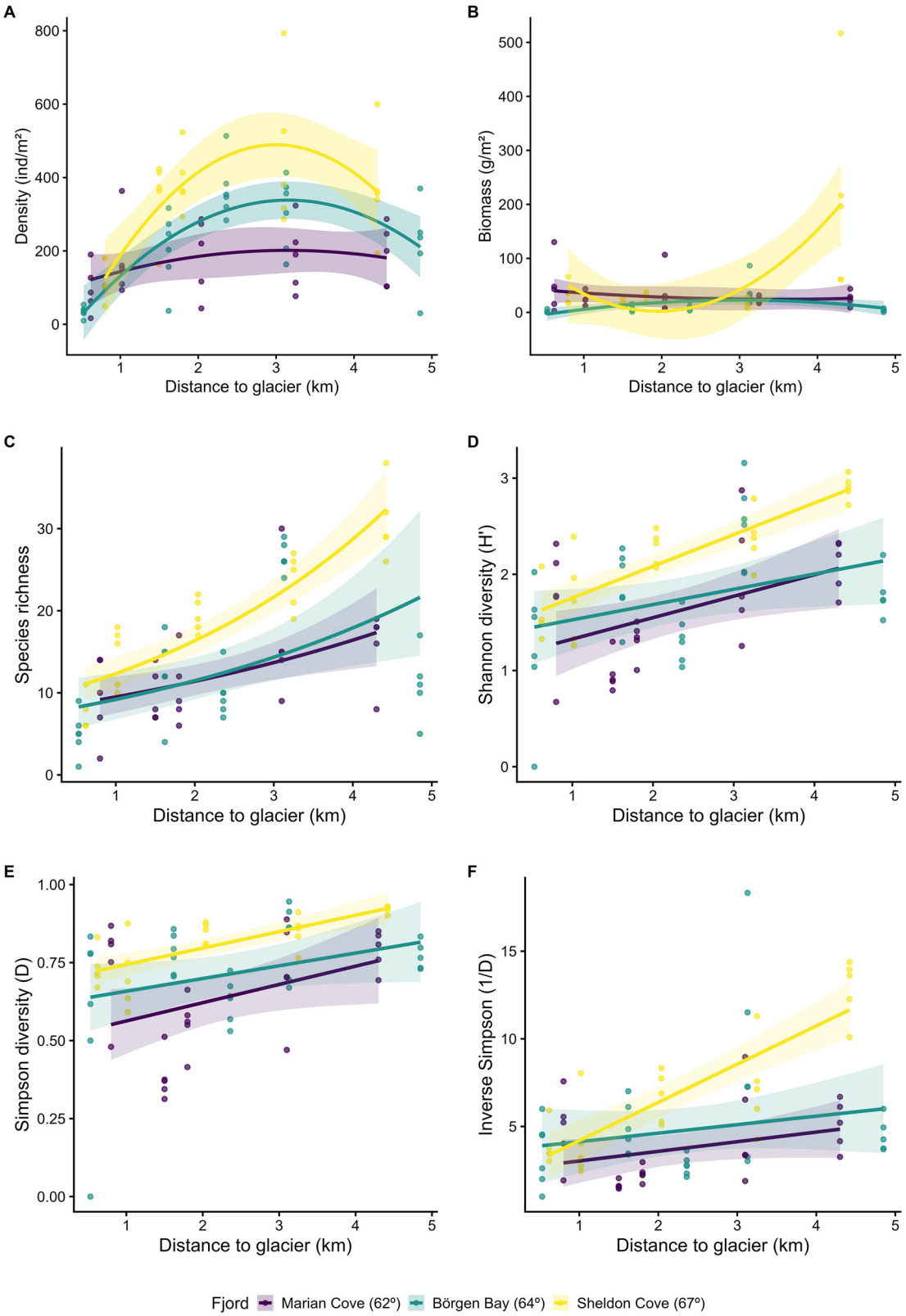


Fig. 6 | Linear and non-linear mixed-effects models (LME, NLME) fitted to describe changes in **A** total density, **B** total biomass, **C** species richness, **D** Shannon diversity, **E** Simpson diversity and **F** inverse Simpson diversity along the distance-to-glacier gradient for the three studied fjords. Given its count-data structure, species richness was analysed using generalised linear mixed models (GLMMs). Points represent replicate-level observations, coloured by fjord, and lines show the fitted model predictions with 95% confidence intervals. Models were fitted using $n = 79$ grab samples: Marian Cove, $n = 25$; Börgen Bay, $n = 29$; Sheldon Cove, $n = 25$.

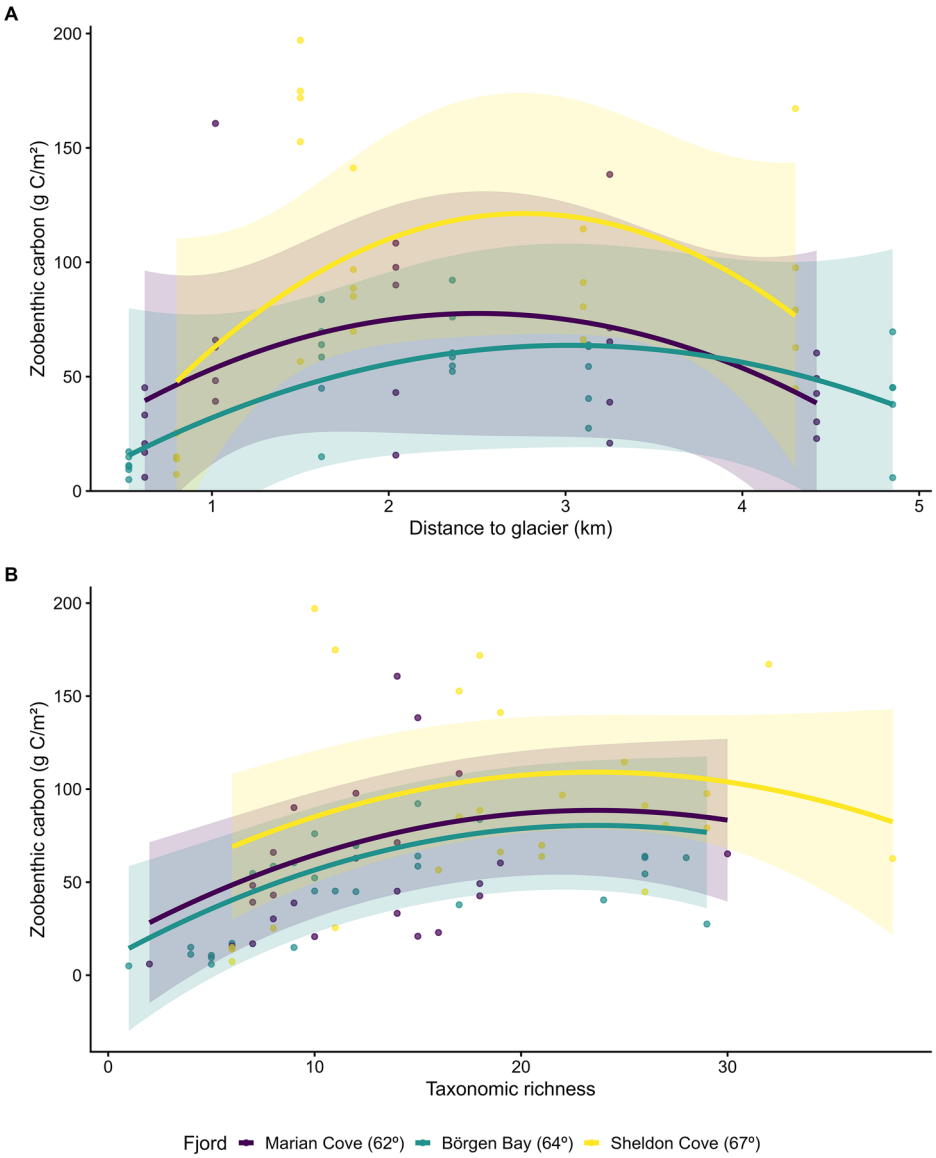


Fig. 7 | Non-linear mixed-effects models (NLME) fitted to describe changes in model-derived zoobenthic carbon (zC) proxy in relation to **A** distance from the glacier and **B** taxonomic richness across the three studied fjords. Points represent replicate-level observations, coloured by fjord and lines show the fitted model predictions with 95% confidence intervals. Models were fitted using $n = 79$ grab samples: Marian Cove, $n = 25$; Börgen Bay, $n = 29$; Sheldon Cove, $n = 25$.

Limitations and future directions

This study presents three principal limitations. First, it provides a spatial snapshot rather than a temporal series, requiring indirect inference of relationships among glacier retreat, hydrographic conditions and benthic assemblage shift from distance-to-glacier gradients and documented retreat histories. Second, the analysis is restricted to soft-sediment macrofauna and epibenthic megafauna, excluding other biological compartments such as meiofauna, microbial assemblages and buried sedimentary carbon. Third, the model-derived zC proxy relies on coefficients originally developed for epifaunal assemblages and thus serves only as a comparative proxy of carbon-storage potential, not as a validated estimate of absolute carbon stock. In the context of Antarctic blue carbon, the quantity of benthic carbon and its relevance for spatial planning depend substantially on the biological compartment assessed and the estimation method employed[27,57]. Although these limitations do not undermine the observed spatial patterns, they restrict extrapolation to whole-fjord biodiversity or carbon budgets. Species accumulation curves and Chao estimators further indicate that inference about total species pools and taxonomic overlap is limited by incomplete detection of low-frequency taxa with patchy occurrence, consistent with known spatial heterogeneity in Antarctic benthos[65,66].

Future research should extend this spatial baseline through temporal monitoring, direct measurements of sedimentation and carbon burial, and refined biomass- and carbon-based estimates for both infaunal and epifaunal assemblages. Such studies should also integrate spatially matched biological assemblage matrices with environmental matrices, including hydrographic, sedimentary and organic-matter variables and analyse these relationships using multivariate or model-based approaches. This would help identify the relative contribution of specific environmental drivers to soft-sediment benthic assemblage structure across Antarctic fjord gradients. Cross-calibration among grab sampling, seabed imagery, sediment eDNA/metabarcoding and direct carbon measurements would enhance comparability and reduce uncertainty, particularly in soft sediments where a significant proportion of fauna may remain undetected in visual surveys[67]. Molecular approaches could expand detection to include meiofauna, protists, fungi and microbial assemblages[68–70], while targeted direct sampling remains essential in understudied polar fjords. The identification of six potentially undescribed species highlights the lack of current biodiversity inventories and emphasises the need for complementary surveys to determine whether newly ice-free habitats develop into more diverse, functionally complex and carbon-rich systems, or remain limited by glacier-derived disturbance as deglaciation progresses[71].

Conclusions

This study provides a comparative assessment of grab-sampled soft-sediment benthic assemblages across multiple Western Antarctic Peninsula fjords with documented glacier retreat. This comparative framework shows that deglaciating Antarctic fjords do not follow a single spatial pattern of ecological variation, but instead develop spatially heterogeneous assemblages across glacier-influenced gradients. The comparison among Marian Cove, Börgen Bay and Sheldon Cove indicates that common signals of glacier influence are likely filtered by local hydrographic and sedimentary conditions, producing contrasting ecological states among fjords. This heterogeneity affects not only taxonomic composition and diversity, but also functional organisation and model-derived carbon-storage potential. By integrating the zC proxy, the study extends biodiversity assessment towards carbon-related ecosystem properties, highlighting the broader functional relevance of benthic assemblage structure in Antarctic coastal systems. Overall, this spatial multi-fjord baseline demonstrates that grab-sampled soft-sediment benthic faunal assemblages can provide a sensitive lens for assessing ecological variation across glacier-influenced Antarctic fjord gradients. Future time-series studies building on this framework will be needed to determine how these assemblages change through time under ongoing environmental change.

Methods

Study locations

In December 2018, the ICEBERGS II research cruise (JR18003) was conducted aboard the RRS *James Clark Ross*. During this expedition, grab samples were used to collect soft-sediment benthic fauna from the seabed of three fjords spaced latitudinally along the Western Antarctic Peninsula: northernmost (Marian Cove, King George Island, South Shetland Islands), intermediate (Börgen Bay, Anvers Island) and southernmost (Sheldon Cove, Adelaide Island) (Fig. 1). The sampled fauna included macrofauna organisms (infauna and epifauna) and epibenthic megafauna retained on the 1 mm sieve during processing. Although all three fjords are glacier-influenced systems with documented retreat, marine- or semi-marine-terminating glacier fronts, and sill structures, they differ substantially in their physical characteristics. Glacier retreat between 1978/79 and 2019 resulted in loss of 1.71 km^2 of glacier area in Marian Cove, 7.81 km^2 in Börgen Bay, and 7.82 km^2 in Sheldon Cove. Marian Cove, influenced by the Fourcade Glacier, is the smallest and shallowest system, measuring approximately 4.5 km in length, 1.5 km in width and ~100–130 m in depth[35]. Börgen Bay, fed by the William Glacier, forms a broader embayment with an approximately 7 km-wide entrance and basin depths of 250–310 m[72]. Sheldon Cove, draining the Sheldon Glacier, is the largest fjord (~13.5 km long and ~2.5 km wide) and is separated from Ryder Bay by a steep sill at ~200 m before descending into basin depths greater than 500 m[35]. The sediment composition of all fjords was sand-dominated. However, Marian Cove contained finer cohesive sandy muds, Börgen Bay featured similar sediments enriched with coarse glacial material, and Sheldon Cove exhibited the broadest range of compositions, from fine sandy muds to clay-rich and gravel-laden substrates[21]. These geomorphological and substrate differences create distinct benthic habitats and environmental gradients that have the potential to shape the biological responses investigated in this study.

Environmental variables

Physical oceanographic conditions at the designated sampling stations were characterised by measuring seawater temperature, salinity, fluorescence (as a proxy for chlorophyll a), and beam transmittance (as a proxy for water turbidity) in December 2018 (Supplementary Table 8). Measurements were obtained through vertical profiling of the water column using a SeaBird 911plus CTD (Conductivity–Temperature–Depth) system, deployed from the research vessel RRS *James Clark Ross*. Salinity was calculated from CTD data, and calibrated against discrete water samples collected using Niskin bottles mounted on the CTD rosette, which were subsequently analysed using an Autosal 8400B salinometer[72].

Oceanographic conditions were characterised by examining the data in potential temperature–salinity (θ–S) space, which elucidates the water masses present and mixing between them. Along-fjord section plots of CTD variables enabled assessment of the influence of glacial melt on the vertical and horizontal structure of the water column in each fjord.

Biological sampling description

In each fjord, a linear transect was established from the edge of the glacier towards the sea along the fjord. Five sampling stations were positioned along this transect at distances of less than 1 km (glacier terminus), 1–2 km, 2–3 km, 3–4 km, and greater than 4 km (fjord mouth) (Fig. 1 and Supplementary Table 9). This design enabled sampling across stations with contrasting degrees of present-day glacier influence and inferred habitat exposure. Stations near the fjord mouth are interpreted as relatively longer-established or less glacier-influenced habitats, whereas stations near the glacier terminus are interpreted as more recently exposed and/or more strongly glacier-influenced habitats. However, this spatial transect was not treated as a formal chronosequence, and differences along the gradient cannot by themselves demonstrate long-term temporal succession.

Benthic samples were collected at all stations using a large Hamon grab with an effective seabed sampling area of approximately 0.30 m^2. This area was estimated from the internal bucket width (0.375 m) and the cutting-edge sweep length during closure (~0.785 m), giving an effective sampled area of ~0.295 m^2. The value was rounded to 0.30 m^2 for area standardisation and to facilitate comparison with previous benthic studies using area-standardised Hamon grab data. The grab was deployed five to six times per station from the starboard side at depths ranging from approximately 90 to 303 m; further details are provided in Supplementary Table 9. Once on deck, the contents were rinsed with seawater and sieved sequentially through a 10 mm sieve to remove large rocks, then through a 1 mm sieve. Fauna and sediment retained on the 1 mm sieve were transferred to the wet laboratory, separated from gravel using tweezers, sorted into major taxonomic groups (such as Phylum or Class), and preserved in pre-labelled bottles containing 98.7% ethanol. The sampled assemblages comprised grab-sampled soft-sediment benthic fauna retained on a 1 mm sieve. Within this material, we distinguished two complementary components. The macrofaunal fraction was defined operationally as infaunal and smaller epifaunal organisms retained during processing, consistent with standard soft-bottom macrofaunal survey practice[28]. Epibenthic megafauna was defined as larger-bodied epifaunal organisms recovered from the Hamon grab samples, including taxa such as ophiuroids, ascidians, asteroids and actiniarians. This usage is consistent with Antarctic benthic studies that define epibenthic megafauna as organisms visible to the naked eye or recognisable in seabed images, commonly around >1 cm[17,26]. Because the material was collected by grab rather than imagery, no fixed upper body-size threshold was applied; instead, the upper size range was constrained by the dimensions and volume of the Hamon grab. Thus, the distinction between macrofauna and epibenthic megafauna was based on ecological position and body size within the grab-retained material, rather than on a strict sieve-based separation between the two components. Hereafter, we refer to these combined components as soft-sediment benthic fauna.

Species identification

Specimens were initially categorised through in-depth examination under a stereomicroscope. This procedure was supplemented by consulting relevant taxonomic references, including recent scientific articles and field guides, to achieve identification at the lowest possible taxonomic level[73–77]. Each morphotype was photographed to create an extensive photographic library. Preliminary identifications were submitted to taxonomic experts for validation and refinement, with photographs provided as visual aids. When needed, the corresponding sample specimens were included with the photographic documentation to support taxonomic evaluation. This consistent approach provided a robust basis for subsequent taxonomic assessments of the Antarctic assemblages.

Faunal categorisation and biodiversity indices

All individuals in the samples were counted and weighed to obtain ethanol-preserved wet mass. Specimens were preserved in 98.7% ethanol from the time of collection in 2018 until biomass measurements were conducted in September 2023. Prior to weighing, each specimen was removed from ethanol and placed on absorbent paper for a standardised 3-min period to remove excess surface ethanol. Specimens were then weighed immediately using an analytical balance. These blotting and weighing procedures were consistently applied to all specimens. As ethanol preservation can influence absolute wet-mass estimates due to preservation-related mass loss and extraction of soluble compounds, biomass values are interpreted as standardised preserved wet-mass estimates. All samples underwent identical protocols for preservation, storage, blotting and weighing. Therefore, preservation effects are unlikely to introduce systematic procedural bias among fjords or distance-to-glacier categories. Raw counts and preserved masses were standardised to the sampled area to estimate density (ind. m^{-2}) and biomass (g wet mass m^{-2}) for each grab replicate.

Subsequently, organisms were assigned to two complementary sets of categories. At the taxonomic level, individuals were grouped into 22 higher taxonomic groups: Actinaria, Amphipoda, Ascidiacea, Asteroidea, Bivalvia, Bryozoa, Echinoidea, Gastropoda, Hexacorallia, Holothuroidea, Hydrozoa, Isopoda, Nemertea, Octocorallia, Ophiuroidea, Ostracoda, Polychaeta, Priapulida, Pycnogonida, Scaphopoda, Sipuncula and Tanaidacea. Functional-group assignment is described in the following subsection.

Alpha diversity was characterised by calculating observed species richness as well as the Shannon, Simpson and inverse Simpson diversity indices. The Shannon index captures both the number of taxa present and the distribution of their abundances. In contrast, Simpson-based metrics assign greater weight to common taxa. The Simpson diversity index used here increases with diversity, with higher values indicating lower dominance. The inverse Simpson index expresses diversity as the effective number of equally common species, facilitating comparisons among assemblages. These complementary indices collectively disentangle the effects of richness, dominance and evenness when comparing assemblages.

Functional group assignment and zoobenthic carbon estimates

Individuals were assigned to one of the 14 functional groups previously defined for Antarctic benthic fauna[9] to facilitate the linkage between assemblage composition, ecological roles and carbon pathways. Each morphospecies was assigned using a standardised combination of three broad trait axes: feeding mode, mobility/habit and body or skeletal structure. Feeding mode distinguished suspension feeders, deposit feeders, grazers, scavengers/predators and taxa with flexible or mixed strategies. Mobility/habit distinguished sessile or attached forms, sedentary or tube-dwelling taxa, crawlers, mobile taxa and burrowers. Body or skeletal structure distinguished soft-bodied, vermiform, shelled or otherwise calcified taxa and arthropod-bodied taxa. Where species-level ecological information was unavailable, assignments were made conservatively using genus-, family- or higher-taxon-level ecological information, supported by morphology and taxonomic identity. The broad taxonomic groups included within each functional group are summarised in Supplementary Table 10, whereas the complete morphospecies-level functional classification is provided in the data repository[78].

Of these 14 functional groups, 13 were widely represented in our dataset: (a) arthropod scavenger/predator, (b) calcareous grazers, (c) climax suspension feeders, (d) crawler deposit feeders, (e) flexible strategy, (f) mobile calcareous scavenger/predator, (g) mobile soft-bodied scavenger/predator, (h) pioneer suspension feeders, (i) sedentary suspension feeders, (j) sessile calcareous scavenger/predator, (k) sessile soft-bodied scavenger/predator, (l) shelled deposit-feeding burrowers and (m) vermiform deposit feeders. A single individual of *Euphausia* sp. was retained in the taxonomic composition dataset and richness estimates, but was not shown as a separate functional group in the summarised functional composition results because it represented a singleton benthopelagic occurrence.

To derive a model-based functional proxy of zoobenthic carbon (hereafter zC proxy), the density of each functional group was summed within each replicate and standardised to density (individuals m^{-2}) by dividing by the sampled area. Densities were then multiplied by previously published Antarctic fauna-specific functional-group coefficients[9], and the resulting values were summed across the 13 represented groups to obtain replicate-level zC proxy values. The functional-group coefficients used here were originally developed for epifaunal assemblages quantified from seabed imagery and have not yet been specifically calibrated for grab-sampled soft-sediment benthic assemblages. Grab sampling therefore provides a broader representation of the soft-sediment assemblage, but the resulting carbon conversion should be interpreted with caution because it extends the coefficients beyond their original calibration context. Accordingly, zC proxy is treated here as a comparative, model-derived indicator of zoobenthic carbon-storage potential among stations, rather than as a validated estimate of absolute carbon standing stock (g C m^{-2}).

Statistical analysis

All statistical analyses were performed in R v4.5.1 (RStudio) at a 95% confidence level ($p < 0.05$). No observations were removed from the dataset. Analyses utilised the following R packages: *vegan*[79], *iNEXT*[80], *pairwiseAdonis2*[81], *lme4*[82], *glmmTMB*[83], *AICcmodavg*[84], *lmerTest*[85], *car*[86] and *performance*[87].

Benthic assemblage composition was analysed using a Bray–Curtis dissimilarity matrix based on fourth–root transformed abundance to reduce the influence of dominant taxa. A two–way crossed permutational multivariate analysis of variance (PERMANOVA) was then conducted to test for differences among fjords (categorical; three levels: Marian Cove, Börgen Bay, Sheldon Cove) and distances (categorical; five levels: Fjord mouth, 3–4 km, 2–3 km, 1–2 km, Glacier terminus). The model included main effects and their interaction. The number of permutations was set at 9999, except for the Distance effect, where permutations were restricted to account for pseudoreplication. Homogeneity of dispersions was evaluated using PERMDISP analyses for both Fjord ($p = 0.02$) and Distance ($p = 0.29$) effects. Pairwise comparisons were conducted using a reduced set of 45 targeted combinations, including within–fjord and across–fjord distances. The multivariate effect size (R^2) was obtained to complement the pairwise results, with darker colours indicating larger effect sizes in heatmaps. SIMPER analysis was used to identify the taxa contributing most to compositional differences between selected groups. Taxa were retained until a cumulative contribution threshold of 25% was reached, as individual contributions beyond this threshold were generally <2%. Retained taxa were visualised with boxplots in the Supplementary Material to show density contrasts between selected sites. Spatial ordination of assemblage composition was represented using Principal Coordinates Analysis (PCoA). Sampling completeness for each fjord was evaluated using the raw species-by-sample count assemblage matrix. Species accumulation curves were generated separately for each fjord, with replicate samples serving as accumulation units. Chao1 richness estimators were derived from pooled raw abundances within each fjord, while Chao2 estimators were based on sample-based incidence matrices. Sampling completeness was quantified as the ratio of observed to Chao-estimated richness. Both abundance-based and incidence-based sample coverage were calculated to differentiate between the completeness of the sampled abundance distribution and the completeness of taxon detection across samples. The terminal accumulation rate was defined as the increase in expected richness per additional sample at the end of each accumulation curve. These analyses facilitated the assessment of inventory completeness and the observed taxonomic overlap among the studied fjords.

Spatial changes in assemblage density, biomass, richness, diversity indices (Shannon, Simpson and inverse Simpson) and zC proxy along the distance-to-glacier gradient were analysed using linear and non–linear mixed effects models (LME, NLME). The relationship between zC proxy and taxonomic richness was analysed separately using mixed-effects models, with richness as the main predictor and fjord and distance to the

glacier included as covariates. Prior to model fitting, assumptions of normality and homogeneity of variances were evaluated. Shapiro–Wilk tests and quantile-quantile (Q–Q) plots on residuals assessed normality, while homoscedasticity was evaluated using the Breusch-Pagan test and visual inspection of residuals[88]. Model selection was based on the corrected Akaike's Information Criterion (AICc), with the model exhibiting the lowest value selected[89]. Candidate models incorporated Distance from the glacier terminus (continuous variable) and Fjord (categorical variable with three levels: Marian Cove, Börgen Bay, Sheldon Cove) as fixed effects. Sampling station (categorical variable with five levels) nested within Fjord was included as a random effect to account for pseudoreplication arising from the sampling design. Marginal R^2 values were calculated for all final mixed-effects models following standard methods[88], to quantify the variance explained by the fixed-effect structure.

Data availability

The datasets generated and analysed during the current study are publicly available in Mendeley Data at https://doi.org/10.17632/s6bcfp9dsj.2.

Code availability

The R and MATLAB scripts used to reproduce the analyses presented in this study are publicly available in the same Mendeley Data repository at https://doi.org/10.17632/s6bcfp9dsj.2.

Received: 24 June 2026; Accepted: 16 October 2026;
Published online: 12 November 2026

References

1. Eayrs, C., Li, X., Raphael, M. N. & Holland, D. M. Rapid decline in Antarctic sea ice in recent years hints at future change. *Nat. Geosci.* **14**, 460–464 (2021).
2. Lai, C.-Y. et al. Vulnerability of Antarctica's ice shelves to meltwater-driven fracture. *Nature* **584**, 574–578 (2020).
3. Dømgaard, M. et al. Half a century of dynamic instability following the ocean-driven break-up of Wordie Ice Shelf. *Nat. Commun.* **16**, 4016 (2025).
4. Cook, A. J. et al. Ocean forcing of glacier retreat in the western Antarctic Peninsula. *Science* **353**, 283–286 (2016).
5. Wallis, B. J. et al. Ocean warming drives rapid dynamic activation of marine-terminating glacier on the west Antarctic Peninsula. *Nat. Commun.* **14**, 7535 (2023).
6. Henley, S. F. et al. Variability and change in the west Antarctic Peninsula marine system: research priorities and opportunities. *Prog. Oceanogr.* **173**, 208–237 (2019).
7. Davies, B. J. et al. The Antarctic Peninsula under present day climate and future low, medium-high and very high emissions scenarios. *Front. Environ. Sci.* **13**, 1730203 (2026).
8. Cauvy-Fraunié, S. & Dangles, O. A global synthesis of biodiversity responses to glacier retreat. *Nat. Ecol. Evol.* **3**, 1675–1685 (2019).
9. Barnes, D. K. A. et al. Blue carbon gains from glacial retreat along Antarctic fjords: What should we expect? *Glob. Change Biol.* **26**, 2750–2755 (2020).
10. Jerosch, K. et al. Benthic meltwater fjord habitats formed by rapid glacier recession on King George Island, Antarctica. *Philos. Trans. R. Soc. Math. Phys. Eng. Sci.* **376**, 20170178 (2018).
11. Valdivia, N., Garrido, I., Bruning, P., Piñones, A. & Pardo, L. M. Biodiversity of an Antarctic rocky subtidal community and its relationship with glacier meltdown processes. *Mar. Environ. Res.* **159**, 104991 (2020).
12. Meredith, M. P. et al. Anatomy of a glacial meltwater discharge event in an Antarctic cove. *Philos. Trans. R. Soc. Math. Phys. Eng. Sci.* **376**, 20170163 (2018).
13. Krause, J. et al. Trace element (Fe, Co, Ni and Cu) dynamics across the salinity gradient in Arctic and Antarctic glacier fjords. *Front. Earth Sci.* **9**, 725279 (2021).
14. Bianchi, T. S. et al. Fjords as Aquatic Critical Zones (ACZs). *Earth-Sci. Rev.* **203**, 103145 (2020).
15. Sahade, R. et al. Climate change and glacier retreat drive shifts in an Antarctic benthic ecosystem. *Sci. Adv.* **1**, e1500050 (2015).
16. Lagger, C., Servetto, N., Torre, L. & Sahade, R. Benthic colonization in newly ice-free soft-bottom areas in an Antarctic fjord. *PLoS ONE* **12**, e0186756 (2017).
17. Kim, D.-U., Ahn, I.-Y., Noh, J., Lee, C. & Khim, J. S. Shifts in benthic megafauna communities after glacial retreat in an Antarctic fjord. *Commun. Earth Environ.* **5**, 438 (2024).
18. Lagger, C. et al. Climate change, glacier retreat and a new ice-free island offer new insights on Antarctic benthic responses. *Ecography* **41**, 579–591 (2018).
19. Bax, N. et al. Perspective: Increasing blue carbon around Antarctica is an ecosystem service of considerable societal and economic value worth protecting. *Glob. Change Biol.* **27**, 5–12 (2021).
20. Morley, S. A. et al. Benthic biodiversity, carbon storage and the potential for increasing negative feedbacks on climate change in shallow waters of the Antarctic Peninsula. *Biology* **11**, 320 (2022).
21. Zwerschke, N. et al. Quantification of blue carbon pathways contributing to negative feedback on climate change following glacier retreat in West Antarctic fjords. *Glob. Change Biol.* **28**, 8–20 (2022).
22. Cape, M. R. et al. Circumpolar Deep Water impacts glacial meltwater export and coastal biogeochemical cycling along the West Antarctic Peninsula. *Front. Mar. Sci.* **6**, 144 (2019).
23. Wlodarska-Kowalczuk, M., Pearson, T. & Kendall, M. Benthic response to chronic natural physical disturbance by glacial sedimentation in an Arctic fjord. *Mar. Ecol. Prog. Ser.* **303**, 31–41 (2005).
24. van der Kamp, A. A. W., González Triginer, V. & Sen, A. Billefjorden's benthic biodiversity: the impact of glacier retreat on faunal communities in a high Arctic fjord. *Polar Biol.* **48**, 71 (2025).
25. Grange, L. J. & Smith, C. R. Megafaunal communities in rapidly warming fjords along the West Antarctic Peninsula: hotspots of abundance and beta diversity. *PLoS ONE* **8**, e77917 (2013).
26. Moon, H.-W., Wan Hussin, W. M. R., Kim, H.-C. & Ahn, I.-Y. The impacts of climate change on Antarctic nearshore mega-epifaunal benthic assemblages in a glacial fjord on King George Island: responses and implications. *Ecol. Indic.* **57**, 280–292 (2015).
27. Pasotti, F. et al. Antarctic shallow water benthos in an area of recent rapid glacier retreat. *Mar. Ecol.* **36**, 716–733 (2015).
28. Rumohr, H. *Soft Bottom Macrofauna: Collection, Treatment, and Quality Assurance of Samples* (1999).
29. Bianchi, T. S. et al. What global biogeochemical consequences will marine animal–sediment interactions have during climate change? *Elem. Sci. Anthr.* **9**, 00180 (2021).
30. Yoo, K.-C., Kyung Lee, M., Il Yoon, H., Il Lee, Y. & Yoon Kang, C. Hydrography of Marian Cove, King George Island, West Antarctica: implications for ice-proximal sedimentation during summer. *Antarct. Sci.* **27**, 185–196 (2015).
31. Kim, Y. et al. Properties and mechanisms of seawater exchange in Marian Cove, King George Island, West Antarctic Peninsula. *J. Geophys. Res. Oceans* **128**, e2023JC020111 (2023).
32. Carroll, D. et al. Modeling turbulent subglacial meltwater plumes: implications for fjord-scale buoyancy-driven circulation. *J. Phys. Oceanogr.* **45**, 2169–2185 (2015).
33. De Andrés, E. et al. Surface emergence of glacial plumes determined by fjord stratification. *Cryosphere* **14**, 1951–1969 (2020).
34. Meredith, M. P. et al. Internal tsunamigenesis and ocean mixing driven by glacier calving in Antarctica. *Sci. Adv.* **8**, eadd0720 (2022).
35. Jones, R. L. et al. Continued glacial retreat linked to changing macronutrient supply along the West Antarctic Peninsula. *Mar. Chem.* **251**, 104230 (2023).

36. Moffat, C. & Meredith, M. Shelf–ocean exchange and hydrography west of the Antarctic Peninsula: a review. *Philos. Trans. R. Soc. A* **376**, 20170164 (2018).
37. Kim, H. et al. Inter-decadal variability of phytoplankton biomass along the coastal West Antarctic Peninsula. *Philos. Trans. R. Soc. A* **376**, 20170174 (2018).
38. Venables, H. J. et al. Sustained, year-round oceanographic measurements from Rothera Research Station, Antarctica, 1997–2017. *Sci. Data* **10**, 265 (2023).
39. Mason, M. et al. Total Organic Carbon, Lead-210, and thermogravimetric analysis data from sediment cores from Marian Cove, Börgen Bay, and Sheldon Cove, December 2018 to January 2020. Preprint at *Zenodo* https://doi.org/10.5281/zenodo.21723066 (2026).
40. Bardi-Puigdefàbregas, P. et al. Stable isotope insights into the habitat use of two benthic invertebrates along Antarctic glacier-influenced fjords. *Mar. Environ. Res.* **220**, 108123 (2026).
41. Smith, C. R., Mincks, S. & DeMaster, D. J. A synthesis of bentho-pelagic coupling on the Antarctic shelf: food banks, ecosystem inertia and global climate change. *Deep Sea Res. Part II Top. Stud. Oceanogr.* **53**, 875–894 (2006).
42. Shim, J., Kang, Y. C., Kang, D.-J. & Han, M. W. Fluxes and budgets of biogenic elements at the sediment-water interface of Marian Cove, King George Island. *Antarct. Sci.* **23**, 358–368 (2011).
43. Braeckman, U. et al. Glacial melt disturbance shifts community metabolism of an Antarctic seafloor ecosystem from net autotrophy to heterotrophy. *Commun. Biol.* **4**, 148 (2021).
44. Braeckman, U. et al. Glacial melt impacts carbon flows in an Antarctic benthic food web. *Front. Mar. Sci.* **11**, 1359597 (2024).
45. Kim, D.-U., Khim, J. S. & Ahn, I.-Y. Patterns, drivers and implications of ascidian distributions in a rapidly deglaciating fjord, King George Island, West Antarctic Peninsula. *Ecol. Indic.* **125**, 107467 (2021).
46. Vause, B. J. et al. Spatial and temporal dynamics of Antarctic shallow soft-bottom benthic communities: ecological drivers under climate change. *BMC Ecol.* **19**, 27 (2019).
47. Stark, J. S., Johnstone, G. & Stark, S. C. Environmental drivers of biodiversity and community structure in marine soft sediments of the Vestfold Hills, East Antarctica. *Antarct. Sci.* **37**, 550–569 (2025).
48. Ziegler, A. F., Cape, M., Lundesgaard, Ø & Smith, C. R. Intense deposition and rapid processing of seafloor phytodetritus in a glaciomarine fjord, Andvord Bay (Antarctica). *Prog. Oceanogr.* **187**, 102413 (2020).
49. Cummings, V. J. et al. Linking Ross Sea coastal benthic communities to environmental conditions: documenting baselines in a spatially variable and changing world. *Front. Mar. Sci.* **5**, 232 (2018).
50. Post, A. L. et al. Environmental drivers of benthic communities and habitat heterogeneity on an East Antarctic shelf. *Antarct. Sci.* **29**, 17–32 (2017).
51. Grimes, C. J. et al. Benthic community heterogeneity on the Eastern Antarctic continental shelf. *Polar Biol.* **48**, 35 (2025).
52. Kędra, M., Pabis, K., Gromisz, S. & Węsławski, J. M. Distribution patterns of polychaete fauna in an Arctic fjord (Hornsund, Spitsbergen). *Polar Biol.* **36**, 1463–1472 (2013).
53. Bascur, M. et al. A paradise for *Maldane sarsi antarctica*: preliminary characterization of the marine soft-bottom fauna of False Bay (Livingston Island, South Shetland Islands, Antarctica). *Antarct. Sci.* **37**, 338–351 (2025).
54. Włodarska-Kowalczuk, M., Renaud, P., Węsławski, J., Cochrane, S. & Denisenko, S. Species diversity, functional complexity and rarity in Arctic fjordic versus open shelf benthic systems. *Mar. Ecol. Prog. Ser.* **463**, 73–87 (2012).
55. Connell, J. H. Diversity in tropical rain forests and coral reefs. *Science* **199**, 1302–1310 (1978).
56. Frinault, B. A. V. & Barnes, D. K. A. Variability in zoobenthic blue carbon storage across a southern polar gradient. *Mar. Environ. Res.* **199**, 106621 (2024).
57. James, K., Macreadie, P. I., Burdett, H. L., Davies, I. & Kamenos, N. A. It's time to broaden what we consider a 'blue carbon ecosystem'. *Glob. Change Biol.* **30**, e17261 (2024).
58. Morley, S. A. et al. Standardising research on marine biological carbon pathways required to estimate sequestration at Polar and sub-Polar latitudes. *Earth Sci. Rev.* **274**, 105372 (2026).
59. Barnes, D. K. A. & Sands, C. J. Functional group diversity is key to Southern Ocean benthic carbon pathways. *PLoS ONE* **12**, e0179735 (2017).
60. Bulmer, R. H. et al. Blue carbon stocks and cross-habitat subsidies. *Front. Mar. Sci.* **7**, 380 (2020).
61. Souster, T. A., Barnes, D. K. A., Primicerio, R. & Jørgensen, L. L. Quantifying zoobenthic blue carbon storage across habitats within the Arctic's Barents Sea. *Front. Mar. Sci.* **10**, 1260884 (2024).
62. Bergagna, L., Lovrich, G., Riccialdelli, L. & Sahade, R. Blue carbon storage in a sub-Antarctic marine protected area. *Sci. Rep.* **14**, 20642 (2024).
63. Boothroyd, A., Adams, V., Alexander, K. & Hill, N. Priority areas for marine protection in the Amundsen and Bellingshausen Seas, Antarctica. *Mar. Policy* **167**, 106232 (2024).
64. Zwerschke, N. et al. Status of polar blue carbon: toward recognition and integration in marine policy. *Glob. Change Biol.* **32**, e71098 (2026).
65. Gutt, J. et al. Benthic communities and their drivers: a spatial analysis off the Antarctic Peninsula. *Limnol. Oceanogr.* **64**, 2341–2357 (2019).
66. Katz, L., Mitchell, E., Danis, B. & Griffiths, H. Microhabitat patchiness structures benthic biodiversity in the Western Antarctic Peninsula. *Ecol. Evol.* **16**, e73392 (2026).
67. Pineda-Metz, S. E. A. & Gerdes, D. Seabed images versus corer sampling: a comparison of two quantitative approaches for the analysis of marine benthic communities in the southern Weddell Sea (Southern Ocean). *Polar Biol.* **41**, 515–526 (2018).
68. Gielings, R. et al. DNA Metabarcoding methods for the study of marine benthic meiofauna: a review. *Front. Mar. Sci.* **8**, 730063 (2021).
69. Pawlowski, J. et al. Environmental DNA metabarcoding for benthic monitoring: a review of sediment sampling and DNA extraction methods. *Sci. Total Environ.* **818**, 151783 (2022).
70. Mazurkiewicz, M. et al. Sediment DNA metabarcoding and morphology provide complementary insight into macrofauna and meiobenthos response to environmental gradients in an Arctic glacial fjord. *Mar. Environ. Res.* **198**, 106552 (2024).
71. Lelièvre, Y., Saucède, T., Pohl, B. & Hourdez, S. You can't protect what you don't know: Strategies for biodiversity inventories in poorly known marine areas facing global changes. *Adv. Mar. Biol.* **101**, 79–104 (2025).
72. Sands, C. J. et al. *Cruise Report RRS James Clark Ross JR18003* (2018).
73. Brueggeman, P. Underwater Field Guide to Ross Island & McMurdo Sound, Antarctica. University of California: San Diego, 1998.
74. Engl, W. Shells of Antarctica. ConchBooks: Hackenheim, 2012.
75. Rauschert, M., Arntz, W., Hempel, G. Antarctic Macrobenthos: A Field Guide of the Invertebrates Living at the Antarctic Seafloor. Wurster Nordseekueste: Arntz & Rauschert Selbstverlag, 2015.
76. Xavier, J. C. et al. *Crustacean Guide for Predator Studies in the Southern Ocean* (Scientific Committee on Antarctic Research, 2020).
77. Drennan, R., Dahlgren, T. G., Linse, K. & Glover, A. G. Annelid fauna of the Prince Gustav Channel, a previously ice-covered seaway on the Northeastern Antarctic Peninsula. *Front. Mar. Sci.* **7**, 595303 (2021).
78. Bascur, M. et al. Marine soft-sediment benthic assemblage, functional-group, zoobenthic carbon proxy, oceanographic data and analysis code from Marian Cove, Börgen Bay and Sheldon Cove,

Western Antarctic Peninsula. Mendeley Data, V2, https://doi.org/10.17632/s6bcfp9dsj.2 (2026).
79. Oksanen, J. et al. *vegan*: *Community Ecology Package* (CRAN, 2018).
80. Hsieh, T. C., Ma, K. H. & Chao, A. iNEXT: an R package for rarefaction and extrapolation of species diversity (Hill numbers). *Methods Ecol. Evol.* **7**, 1451–1456 (2016).
81. Martinez Arbizu, P. pairwiseAdonis: Pairwise multilevel comparison using *adonis* (2020).
82. Bates, D., Mächler, M., Bolker, B. & Walker, S. Fitting linear mixed-effects models using *lme4*. *J. Stat. Softw.* **67**, 1–48 (2015).
83. Brooks, M. E. et al. glmmTMB balances speed and flexibility among packages for zero-inflated generalized linear mixed modeling. *R. J.* **9**, 378–400 (2017).
84. Mazerolle, M. J. *AICcmodavg: Model selection and multimodel inference based on (Q)AIC(c)* (CRAN, 2023).
85. Kuznetsova, A., Brockhoff, P. B. & Christensen, R. H. B. *lmerTest: tests in linear mixed effects models*. Version 3, 2–1 https://doi.org/10.32614/CRAN.package.lmerTest (2013).
86. Fox, J., Weisberg, S. & Price, B. *Car: Companion to Applied Regression*. Version 3, 1–5 https://doi.org/10.32614/CRAN.package.car (2001).
87. Lüdecke, D., Ben-Shachar, M. S., Patil, I., Waggoner, P. & Makowski, D. *performance*: an R package for assessment, comparison and testing of statistical models. *J. Open Source Softw.* **6**, 3139 (2021).
88. Zuur, A. F., Ieno, E. N., Walker, N., Saveliev, A. A. & Smith, G. M. *Mixed Effects Models and Extensions in Ecology with R*. https://doi.org/10.1007/978-0-387-87458-6 (Springer, 2009).
89. Nakagawa, S., Johnson, P. C. D. & Schielzeth, H. The coefficient of determination R^2 and intra-class correlation coefficient from generalized linear mixed-effects models revisited and expanded. *J. R. Soc. Interface* **14**, 20170213 (2017).
90. Cook, A., Fox, A. & Thomson, J. Coastal change data for the Antarctic Peninsula region, 1843 to 2008. 2 files, 37 MB NERC EDS UK Polar Data Centre. https://doi.org/10.5285/07727663-9B94-4069-A486-67E4D82177D3 (2021).

Acknowledgements

We thank all crew members, technicians and researchers who participated in the ICEBERGS Antarctic campaigns (2017–2020) on board the RRS *James Clark Ross* for their support with sampling and sample processing. We are especially grateful to the taxonomic experts who assisted with specimen identification: Dr Álvaro Peña (Hydrozoa), Dr Anna Jażdżewska (Amphipoda), Dr Anna Soler (Pycnogonida), Dr Camille Moureau (Asteroidea), Dr Chester Sands (Ophiuroidea), Dr Declan Morrissey (Octocorallia), Dr Estefanía Rodríguez (Actinaria, Zoantharia), Dr José Ignacio Saiz-Salinas (Priapulida, Echiura, Sipuncula), Dr Katrin Linse (Bivalvia, Scaphopoda), Dr Melanie Mckenzie (Holothuroidea), Dr Natsumi Hookabe (Nemertea), Dr Ricardo Sahade and Dr Marcos Tatián (Ascidiacea), Dr Sebastián Rosenfeld (Gastropoda), Dr Stephanie Kaiser (Isopoda, Tanaidacea), Dr Stephen Cairns (Hexacorallia) and Dr Thomas Saucède (Echinoidea). M.B. thanks Dr Sara Garcia-Ravelo for laboratory support and Andrea Prófumo and Pau Bardi-Puigdefàbregas for guidance with QGIS and Quantarctica during map creation. This study contributes to the 'Integrated Science to Inform Antarctic and Southern Ocean Conservation' (Ant-ICON) research programme of the Scientific Committee on Antarctic Research (SCAR).

Author contributions

Miguel Bascur: Conceptualisation, Data curation, Formal analysis, Investigation, Methodology, Software, Validation, Visualisation, Writing—original draft, Writing—review & editing. **Stuart Jenkins**: Funding acquisition, Conceptualisation, Resources, Investigation, Supervision, Writing—review & editing. **Michael P. Meredith**: Funding acquisition, Investigation, Visualisation, Writing—review & editing. **Katy Sheen**: Investigation, Visualisation, Writing—review & editing. **Carlos P. Muñoz-Ramírez**: Investigation, Methodology, Data curation, Writing—review & editing. **Kate Retallick**: Investigation, Writing—review & editing. **Antonio Brante**: Funding acquisition, Investigation, Project administration, Resources, Writing—review & editing. **João Gil**: Investigation, Methodology, Writing—review & editing. **Conxita Avila**: Funding acquisition, Investigation, Project administration, Resources, Supervision, Writing—review & editing. **David K.A. Barnes**: Conceptualisation, Funding acquisition, Investigation, Project administration, Resources, Supervision, Writing—review & editing.

Funding

Sampling was funded by the ICEBERGs research project (N° PII20150078), a joint collaboration between the Ministerio de Ciencia, Tecnología, Conocimiento e Innovación of Chile and the Natural Environment Research Council of the United Kingdom. This work was also supported by the CHALLENGE (PID2019-107979RB-100 funded by MICIU/AEI/10.13039/501100011033) and CHALLENGE-2 (PID2022-141628NB-I00 funded by MICIU/AEI/10.13039/501100011033) research grants from the Spanish Government, with partial support from the European Regional Development Fund (ERDF-EU). The 'Marine Biodiversity and Evolution' SGR Research Quality Group of the Generalitat de Catalunya (MBE; 2021SGR01271) also supported this work. M.B. acknowledges financial support from Agencia Nacional de Investigación y Desarrollo (ANID), Becas Chile para Doctorado en el extranjero N° 72220140. K.S. acknowledges funding from the British Antarctic Survey CASS fund, which supported her participation in the ICEBERGS II cruise, during which she processed and calibrated the CTD data. J.G. was supported by an ongoing collaborative agreement signed with CREOCEAN (France).

Competing interests

The authors declare no competing interests.

Additional information

Supplementary information The online version contains supplementary material available at https://doi.org/10.1038/s43247-026-04216-1.

Correspondence and requests for materials should be addressed to Miguel Bascur.

Peer review information *Communications Earth & Environment* thanks all reviewers for their contribution to the peer review of this work. Primary handling editor: Nadine Schubert and Marisa McDonald.

Reprints and permissions information is available at http://www.nature.com/reprints

Publisher's note Springer Nature remains neutral with regard to jurisdictional claims in published maps and institutional affiliations.

Open Access This article is licensed under a Creative Commons Attribution-NonCommercial-NoDerivatives 4.0 International License, which permits any non-commercial use, sharing, distribution and reproduction in any medium or format, as long as you give appropriate credit to the original author(s) and the source, provide a link to the Creative Commons licence, and indicate if you modified the licensed material. You do not have permission under this licence to share adapted material derived from this article or parts of it. The images or other third party material in this article are included in the article's Creative Commons licence, unless indicated otherwise in a credit line to the material. If material is not included in the article's Creative Commons licence and your intended use is not permitted by statutory regulation or exceeds the permitted use, you will need to obtain permission directly from the copyright holder. To view a copy of this licence, visit http://creativecommons.org/licenses/by-nc-nd/4.0/.

© The Author(s) 2026

This Article in Press is shared early to give you faster access to new research. It is citable and carries a permanent DOI. The final edited version will replace it automatically.